



Close temporal correspondence between geomagnetic anomalies and earthquakes during the 2002–2003 eruption of Etna volcano

G. Currenti,¹ C. Del Negro,¹ M. Johnston,² and Y. Sasai³

Received 5 March 2007; revised 28 May 2007; accepted 18 June 2007; published 12 September 2007.

[1] The early stages of the 2002–2003 lateral eruption at Mount Etna were accompanied by slow changes (over some hours) and some rapid step offsets in the local magnetic field. At five monitoring locations, the total magnetic field intensity has been measured using continuously operating Overhauser magnetometers at a sampling rate of 10 s. The very unique aspect of these observations is the close temporal correspondence between magnetic field offsets and earthquakes that occurred in the upper northern flank of the volcano on 27 October 2002 prior to a primary eruption. Rapid coseismic changes of the magnetic field were clearly identified for three of the most energetic earthquakes, which were concentrated along the Northeast Rift at a depth of about 1 km below sea level. Coseismic magnetic signals, with amplitudes from 0.5 to 2.5 nT, have been detected for three of the largest seismic events located roughly midway between the magnetic stations. We quantitatively examine possible geophysical mechanisms, which could cause the magnetic anomalies. The comparison between magnetic data, seismicity and surface phenomena implies that piezomagnetic effects are the primary physical mechanism responsible for the observed magnetic anomalies although the detailed cause of the rapid high stress change required is not clear. The modeling of the observed coseismic magnetic changes in terms of piezomagnetic mechanism provides further evidence of the complex interaction between volcanic and tectonic processes during dike propagation along the Northeast Rift.

Citation: Currenti, G., C. Del Negro, M. Johnston, and Y. Sasai (2007), Close temporal correspondence between geomagnetic anomalies and earthquakes during the 2002–2003 eruption of Etna volcano, *J. Geophys. Res.*, *112*, B09103, doi:10.1029/2007JB005029.

1. Introduction

[2] During the past few decades, we have seen a remarkable increase in the quality and quantity of magnetic data recorded before and during volcanic eruptions on Mount Etna. Detection of local magnetic field changes has often been proposed for monitoring the modifications in the stress field or the thermodynamic state within the volcanic edifice [Del Negro and Napoli, 2004]. The most significant recent changes in the local magnetic field were observed at the onset of the 2002–2003 flank eruption on Mount Etna. Preceded by surprisingly little warning (clear seismicity began only two hours before the onset of eruptions), the eruption started early on 27 October 2002 from two fissures on the northeast and south flanks of the volcano, feeding explosive activity and two distinct lava flows (Figure 1). After local differential magnetic field measurements were filtered from the external noise

using adaptive filters, slow changes (over some hours) and rapid step offsets were detected in the data recorded at two sites (PDN and DGL) placed on the northeast flank of volcano [Del Negro *et al.*, 2004]. Unfortunately, the ash emissions and lava flows entirely buried the magnetic stations (BCN, BVD, and CST) located on the south flank and the data were completely lost.

[3] The slow magnetic changes accompanying the onset of the 2002–2003 eruption of Mount Etna have previously been described by Del Negro *et al.* [2004]. They identified two stages in the total intensity changes, which have been closely related to two different volcanic events: (1) a decrease of about 4–5 nT associated with 26 October seismic swarm recorded beneath the summit craters and (2) an increase of 9–10 nT coincident with 27 October eruptive fissures opening up in the north flank [Del Negro *et al.*, 2004; Lanza and Meloni, 2006]. These observations are generally consistent with those calculated from simple magnetic models of these volcanic processes, in which the magnetic changes are produced by stress redistribution due to magmatic intrusions at different depths. The space-time evolution of magnetic data not only allows the timing of the intrusive event to be described in greater detail but also, together with other volcanological and geophysical data, permits some constraints to be placed on the characteristics of propagation

¹Istituto Nazionale di Geofisica e Vulcanologia, Sezione di Catania, Catania, Italy.

²U.S. Geological Survey, Menlo Park, California, USA.

³Disaster Prevention Division, Tokyo Metropolitan Government, Tokyo, Japan.

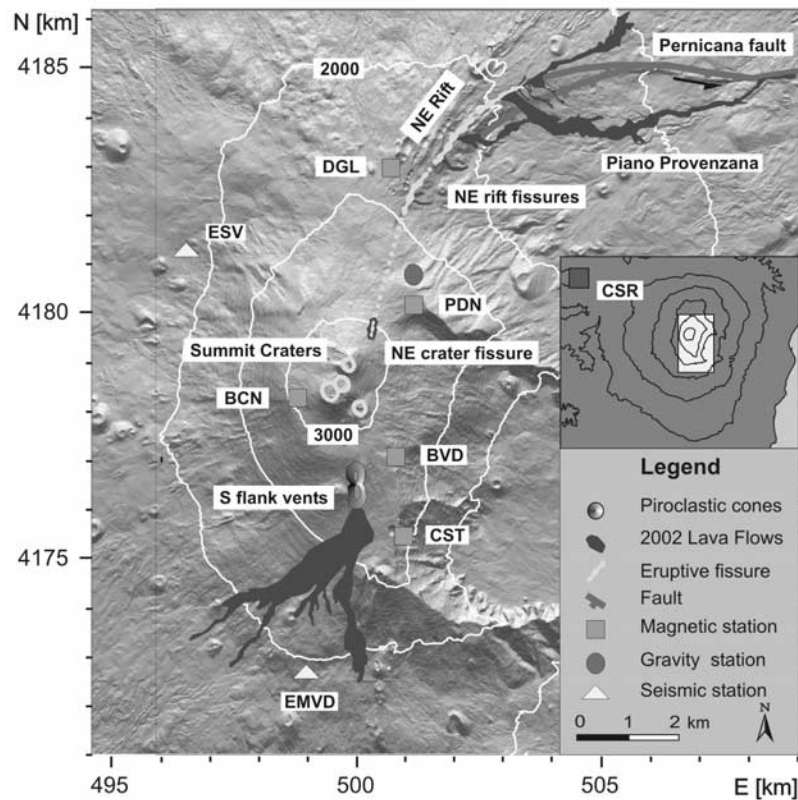


Figure 1. Schematic map showing the area affected by the 2002–2003 Etna eruption. Locations of magnetic stations are shown as squares. Inset shows the position of the reference magnetic station (CSR) installed about 50 km away from the volcanic edifice.

of a shallow dike on the Northeast Rift. In particular, the rate of growth of the magnetic anomalies leads to the interpretation that the magmatic intrusion propagated northward from the base of the Northeast Crater to the Northeast Rift at approximately 14 m min^{-1} [Del Negro *et al.*, 2004].

[4] In this paper, we focus on the rapid magnetic field offsets that have not yet been discussed. Outstanding magnetic changes are well correlated with seismic activity related to the opening of eruptive fractures. Comparison of local magnetic field with the record of seismic events that occurred during the eruption onset shows a close temporal correspondence between the magnetic field offsets and the most energetic earthquakes (Figure 2). These observations were possible only because at each monitoring site, the total magnetic field intensity has been measured using continuously recording Overhauser magnetometers at a resolution of 0.01 nT and a sampling rate of 10 s (unusual for volcano magnetic monitoring). However, the causal relation between observed local magnetic field changes and complex volcanic activity is not yet clearly established, and more than one mechanism may be involved [Del Negro and Currenti, 2003]. We investigate possible source mechanisms that could have produced the rapid magnetic changes. Our aim is to provide a quantitative estimate of the observed magnetic field offsets in order to gain insight into the relation-

ship between local magnetic field changes and volcanic earthquakes.

2. Magnetic Observations

[5] During the night of 26–27 October 2002, the opening of two eruptive fracture systems on the northeast and south flanks of the Mount Etna was accompanied and followed by an intense seismic sequence mainly affecting the eastern sector of the volcanic edifice. A total of 874 earthquakes, with $M > 1.0$, were recorded during the eruption. Seismicity decayed over about two weeks and most of the seismic energy was released during the first 4 days (470 events on a total of 874). A number of earthquakes, during the first hours on 27 October 2002, took place in the central upper part of Mount Etna and several hours later powerful lava fountains and ash columns occurred on the south flank, along a north–south fracture field. In the following hours, the eruptive fracture system on the northeastern flank opened, nearly to the Northeast Rift [Barberi *et al.*, 2004]. The seismicity was mainly related to the magma intrusion along the Northeast Rift, with the highest seismic releases associated with the activation of the Pernicana fault, which is a local tectonic feature. Most of the earthquakes were shallow, being confined in a seismogenic layer ranging from 0 to 7 km below the surface.

[6] In the early morning of 27 October, 12 earthquakes greater than $M3.3$ occurred along the Northeast Rift. Of

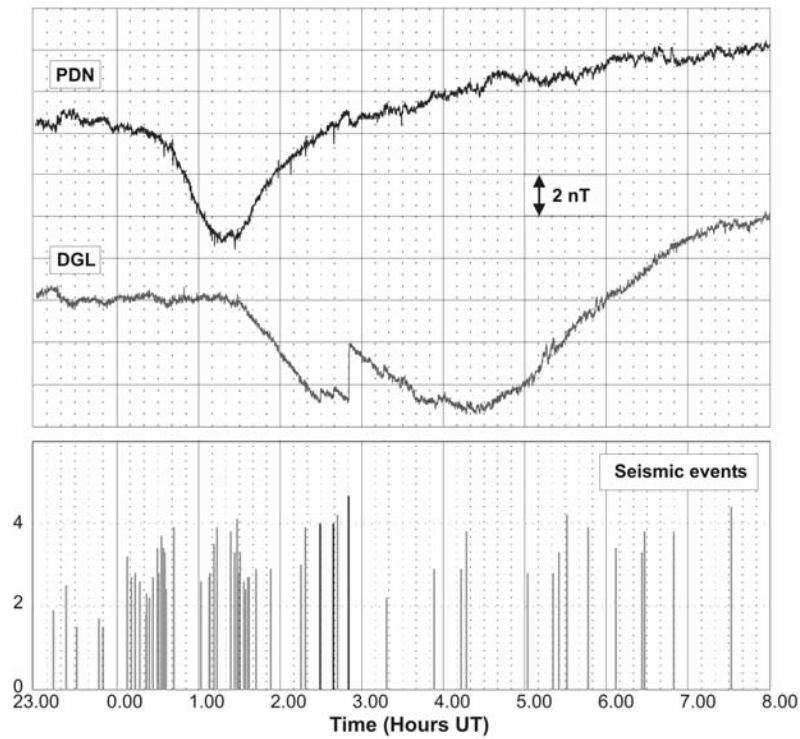


Figure 2. (top) Magnetic field variations at DGL and PDN with respect to the CSR reference station and (bottom) magnitude of seismic events between 26 October at 2300 UT and 27 October at 0800 UT. The seismic events recorded at the time of step-like magnetic changes are shown in black.

these 12 earthquakes, 4 were located roughly midway between the magnetic stations (PDN and DGL), with a focal depth of 1 km below sea level, and of these four events, three were accompanied by rapid magnetic field changes. The magnetic anomalies related to seismic activity were opposite in sign to the field decrease at DGL that started about an hour later than that at PDN during the seismic swarm. For all the examined seismic events the total intensity magnetic changes show clear positive steps at DGL and almost null but slightly negative at PDN (Figure 2). A step change of about 2.5 nT was recorded at the DGL station at the time of the large seismic event at 0250 UT, simultaneous with a step of opposite sign at PDN of -0.6 nT (using 10 s readings). Further positive steps of 0.5 nT occurred at DGL at the times of other large seismic events at 0229 and 0239 UT.

[7] The epicenters of the earthquakes recorded on 27 October in the upper northern flank of the edifice are shown in Figure 3. Earthquakes have been located with a 3D velocity model proposed by *Aloisi et al.* [2002] using the SimulPS12 code [*Evans et al.*, 1994], and the relative fault plane solutions, determined using the FPFIT algorithm [*Reasenber and Oppenheimer*, 1985]. The seismic events are concentrated along the Northeast Rift and show predominant left-lateral strike-slip and reverse dip-slip movements [*Barberi et al.*, 2004]. This kind of kinematics is in agreement with the structural lineaments of the Northeast Rift.

[8] Some important equations in seismology provide a theoretical basis for the source scaling relations. The seismic moment M_o (in N m) was related to the magnitude M and

the source parameters by the following relations [*Hanks and Kanamori*, 1979]:

$$\log_{10} M_o \approx \frac{3}{2} M_L + 9.1 \quad (1)$$

$$M_o = \mu AD \quad (2)$$

where μ is the shear modulus of the crust (in Pa), A is the area of the fault rupture (in m^2), and D is the average

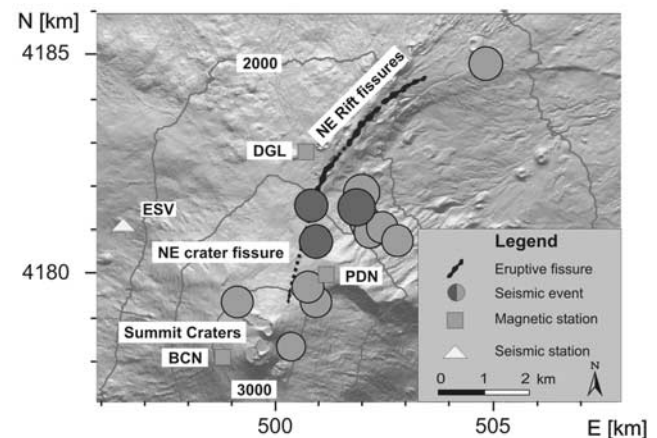


Figure 3. Epicenters of most energetic earthquakes ($M_L > 3.5$) and their focal mechanisms recorded on 27 October 2002.

Table 1. Values of Seismic Parameters of Recorded Events on 27 October 2002 for Stress Drop Ranges From 1 to 100 MPa^a

Seismic Event Time, UT	M_L	Depth, km	Rupture Area, km ²
0229	4.0	0.76	0.1–2.1
0239	4.0	0.71	0.1–2.1
0250	4.8	1.78	0.6–13

^aSee Azzaro *et al.* [2006] and D'Amico and Maiolino [2005].

displacement over the rupture surface (in m). For the crust, a typical value of μ is 30 GPa. For small and moderate magnitude earthquakes (e.g., $M < 6$), the circular rupture and the static stress drop at the center of the rupture are given by [Kanamori and Anderson, 1975; Hough, 1996]

$$\Delta\sigma = \frac{7}{16}\pi^{1.5}\mu\frac{D}{\sqrt{A}} \quad (3)$$

where $\Delta\sigma$ is in Pa. An earthquake mechanism study on Mount Etna shows that the stress drop, accompanying earthquakes having the same order of magnitude, ranges between 1 and 100 MPa [Mulargia *et al.*, 1985]. The results of this study allow us to relate the magnitude of the three seismic events to their physical properties. For the events reported above, we estimated the seismic moment (M_0) and expected fault area values (A), whose ranges are dependent on the assumed stress drop (Table 1).

[9] In order to show that the magnetic field offsets are not changes resulting from the effects of earthquake shaking, we computed the displacements associated with the most energetic seismic events on the basis of the estimated source parameters. For all the considered earthquakes, the ground deformation cannot exceed 1 cm in the horizontal components and 10 cm in the vertical uplift. Since the monitoring sites have low magnetic gradient (less than 2–3 nT m⁻¹ at the sensor height of about 4 m) and low local noise amplitude [Del Negro *et al.*, 2002], we can rule out the physical motion of the sensors from earthquake shaking as the cause of the rapid step offsets recorded in the local magnetic field.

[10] The observed coseismic magnetic offsets are likely to be caused by the stress field changes in the crust associated with the dike intrusion and earthquakes. Short-term variations (from seconds to days) could arise from instantaneous variations of rocks magnetization, induced by local stress redistribution and from fluid flow current through fissures within the volcanic edifice, accompanying fault ruptures and fracture opening. We have been quantitatively investigating possible physical mechanisms, which could generate magnetic signals large enough to account for these observations.

3. Magnetic Anomalies Interpretations

[11] The primary mechanisms involved in generating short-term changes in local magnetic fields include electrokinetic effects and piezomagnetism. We examine each of these mechanisms to determine whether they are likely to explain the observed magnetic anomalies. On the basis of the scaling relationship, it is possible to make an order of magnitude estimate about the amplitude of the magnetic

anomaly expected at the occurrence time of the seismic events [Karakelian *et al.*, 2002].

3.1. Electrokinetic Model

[12] Assuming model parameters derived from inversions of seismic data, the electrokinetic effect expected at the ground surface was computed by using the Murakami [1989] formulation. He devised analytic solutions for computing magnetic fields due to an inclined rectangular fault separating two media with different streaming potential coefficients, $C1$ and $C2$. The electrokinetic source intensity caused by a pore pressure P is quantified by $S = (C1 - C2)P$ and it is constant and bounded by the fault geometry. No source exists outside of this region. A rough order of magnitude estimate of the pore pressure change is evaluated using the seismic stress drop. The fault area was estimated from seismological observations and the model parameters are listed in Table 2. Data on the streaming potential coefficient $C = -(\varepsilon\zeta/\eta\sigma)$, where ε is the dielectric constant of the fluid, ζ is the zeta potential, η is the viscosity of the fluid, and σ is the electrical conductivity, are poorly known. According to experimental results and theoretical studies [Zlotnicki and Le Mouel, 1990; Fenoglio *et al.*, 1995], the streaming potential coefficient of various rocks can vary between 10^{-4} and 4×10^{-3} mV Pa⁻¹ [Zlotnicki and Nishida, 2003]. The difference in the streaming potential coefficient is assumed to be on the order of 10^{-6} V Pa⁻¹. This, considering a seismic stress drop of few megapascals as an indicator of the stress change, could lead to a source intensity of $S = 1$ V.

[13] The maximum amplitude of the magnetic anomaly resulting from this source is not greater than a few tenths of a nanotesla (Figure 4). Moreover, the sign of the expected magnetic anomaly is opposite to that observed and no remarkable variations followed the coseismic step in the total magnetic intensity field. It is worth noting that fluid diffusion takes time and there is no indication of diffusion like character in the magnetic signal that might suggest a fluid-related electrokinetic effect [Johnston, 1997]. Altogether, the observed step-like character of the data is inconsistent with a fluid flow mechanisms, the large observed amplitudes compared to that expected, and the reverse sign of the observed anomalies. This led us to discount the electrokinetic-magnetic effect as a possible source for these events. Magnetic field changes produced by electrokinetic effects should also have associated electric fields. Unfortunately, no electric data were available to be jointly discussed and modeled with the magnetic changes,

Table 2. Summary of Fault Parameters Used in the Electrokinetic Model^a

Parameter	Value
Northing, m	4,181,874
Easting, m	501,849
Depth, km	0.2
Length, km	1
Width, km	1
Strike about north	20°
Dip	45°
Source, V	1

^aThe parameter $\sigma_1 = \sigma_2 = 0.006$ S m⁻¹, inclination 53.3°, declination 1.8°.

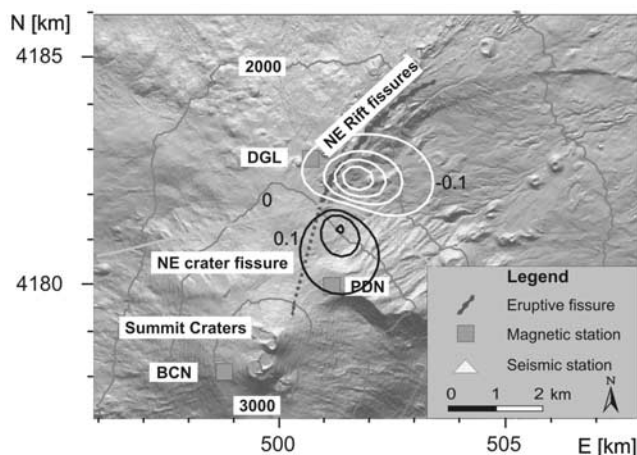


Figure 4. Contour map (at 0.1 nT intervals) of the computed magnetic anomaly produced by the electrokinetic effect model. The source parameters are reported in Table 2.

and the exclusion of the electrokinetic effect as a candidate source process relies entirely upon the indirect field and geological evidence discussed above. Therefore it is difficult to explain the magnetic variations in terms of an electrokinetic fault model.

3.2. Piezomagnetic Model

[14] The amplitude and the timescale of the volcanomagnetic steps could also result from piezomagnetic effects. The fact that rapid steps in the magnetic field occurred coseismically indicates that the magnetic changes are likely caused by stress changes accompanying the events. The stress response was controlled by interactions between volcanic and tectonic processes and was dominated by fast stress propagation and reorientation [Barberi *et al.*, 2004]. The combined effect of vertical intrusion in the upper part of the volcano and radial intrusions in the lower part gave rise to (1) a rotation of the stress tensor [Barberi *et al.*, 2004] and (2) a change in the dike propagation time (Figure 5). The rate of seismic events showed that the dike intrusion in the Northeast Rift occurred with different velocity in the upper and lower part of the fracture system. The change in the

characteristics of the dike propagation was also reported from other geophysical observations [Andronico *et al.*, 2005; Branca *et al.*, 2003]. Changes in the rate of magnetic data [Del Negro *et al.*, 2004] and tilt variations at PDN accompanying the intrusions activity were also estimated (Figure 6). The upper part of the fractures (up to 2400 m elevation) did not erupt lava, whereas the lower fissures (from 2400 to 1900 m) fed a flank eruption. The transition from simple dike propagation to explosive and effusive activity was marked by strong explosive activity and occurrence of the most energetic earthquakes during which step-like variations in the magnetic signals were detected.

[15] It is worthwhile noting that all the step-like magnetic variations at DGL are opposite in sign to the negative trend associated with intrusion activity that characterizes the magnetic anomaly at DGL until about 0430 UT [Del Negro *et al.*, 2004]. This clearly indicates that another associated mechanism was in play besides the tensile opening generated by the intruding dike. Indeed, reverse slip of the preexisting tectonic structures could have been encouraged by dike propagation into the lower part of the Northeast Rift. This follows because the magmatic overpressure of the dike generates a horizontal compressive stress which, in turn, produces shear stress favoring reverse slip on the preexisting boundary faults. When the magmatic overpressure is high (i.e., several tens of megapascals), this horizontal compressive stress can temporarily become the maximum principal compressive stress at shallow depths in rift zones [e.g., Gudmundsson, 2000]. The reverse slip could be maintained on the faults until the compressive and shear stresses generated by the magmatic overpressure are eventually relaxed [Gudmundsson and Loetveit, 2005]. Therefore the opening dike may have caused dip-slip motion of the Northeast Rift zone structures during the early stages of deformation as a mechanical consequence of the interaction between volcanic and tectonic processes. Unfortunately, seismic sequences spanning the analyzed period are not of sufficient quality (many event onsets occurred in the codas of previous events) to use standard inversion techniques to univocally determine the focal mechanism associated with each analyzed seismic event. Indeed, geodetic data inversion show a change in the characteristic of the dike behavior [Aloisi *et al.*, 2006] at the time of the transition from pure dike propagation to

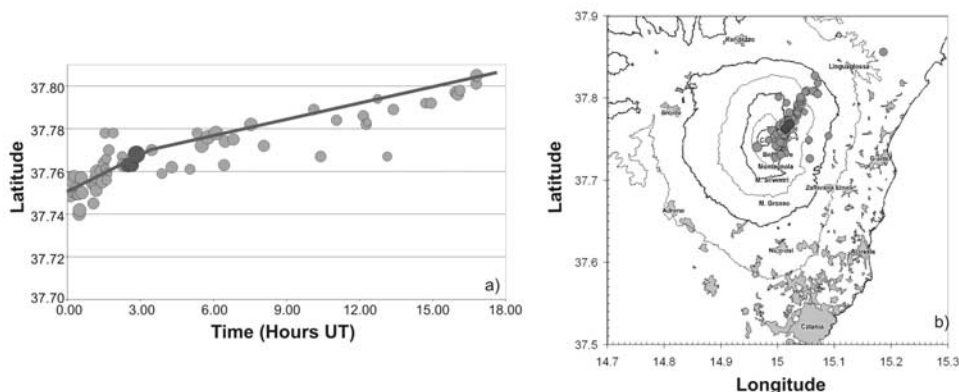


Figure 5. Patterns of the (a) spatial and (b) temporal epicenter location of the seismic events. The black circles represent the seismic events that correspond with the magnetic anomalies.

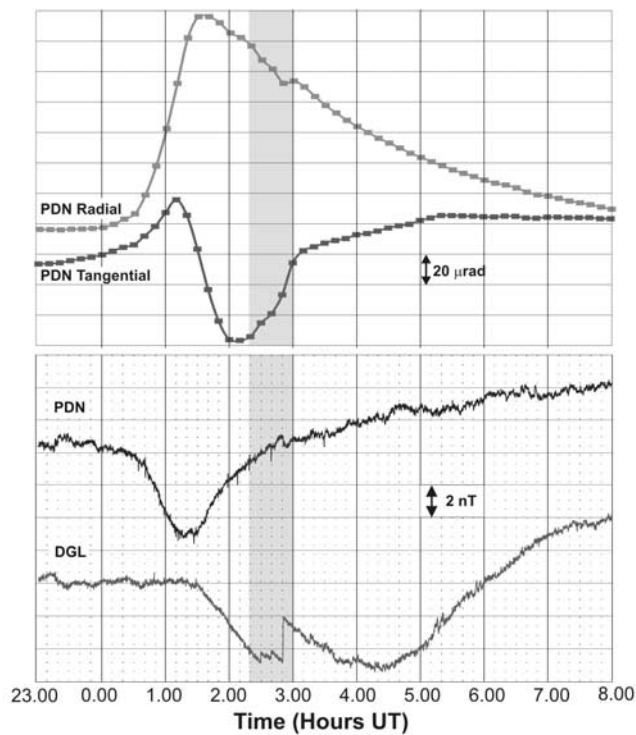


Figure 6. (top) Radial and tangential tilt components recorded at the long-base tilt station located at the Pizzi Deneri Observatory [Aloisi *et al.*, 2003]. (bottom) Magnetic changes at PDN and DGL with respect to the CSR reference station.

effusive activity. A composite tabular dislocation model with tensile opening (3.31 m), dip-slip (3.16 m), and strike-slip (0.81 m) components was derived to explain the continuous tilt data by Aloisi *et al.* [2006, Table 3].

[16] Piezomagnetic models were thus investigated that compute the coseismic magnetic changes expected at the ground surface. According to Utsugi *et al.* [2000], an inclined thrust fault (Table 3) embedded in a homogeneous half-space medium, can produce enough observable magnetic field with a sign consistent with that expected from reverse faulting seismic events (Figure 7). Magnetic model parameters were chosen to be consistent with the location and magnitude of the seismic events. A dip value of 45° was chosen that is in agreement with ground deformation data inversion [Aloisi *et al.*, 2006] and with leveling data recorded along the Pernicana fault [Obrizzo *et al.*, 2001]. However, on the basis of the seismological information (Table 1), the computed piezomagnetic anomaly underestimates by about a factor of 10 the amplitude of the magnetic change observed at DGL in correspondence of the most energetic seismic event (0250 UT).

[17] The amplitude of the expected piezomagnetic anomalies could be affected by the presence of nonuniform rock magnetization and elasticity [Okubo and Oshiman, 2004]. This is probably pertinent to conditions on Mount Etna where both geological data and seismic tomography evidence the presence of severe medium heterogeneities [Patané *et al.*, 2006]. The stress changes are very sensitive to the elastic properties of the medium. Zhao *et al.* [2004]

Table 3. Summary of Fault Parameters Used in The Piezomagnetic Models^a

Parameter	Value
Northing, m	4,181,874
Easting, m	501,849
Depth, km	0.2
Length, km	1.3
Width, km	1.3
Strike about north	20°
Dip	45°
Tensile opening, m	0
Dip slip, m	0.2
Strike slip, m	0

^aMagnetization 2.5 A m^{-1} , inclination 53.3° , declination 1.8° , and sensitivity 10^{-9} Pa^{-1} .

show that rigidity layering can affect the magnitude and the pattern of the stress field. Since the stress-induced magnetization is proportional to the stress field on the basis of linear piezomagnetic theory, the assumption of medium homogeneity could be critical in the investigations of piezomagnetic anomalies. Taking this into account, a piezomagnetic mechanism acting in a heterogeneous layered medium could explain the large magnetic jump at DGL station at the time of the 0250 UT seismic event.

[18] We could also satisfy the amplitude of the magnetic anomaly by increasing some model parameters (i.e., the rupture area or the dislocation parameter), such as might be produced by accompanying aseismic deformation. That would enhance the piezomagnetic anomaly but would also lead to a seismic moment much higher than the estimated one. Seismic moment analyses have recently been revised to better characterize the 0250 UT seismic event (H. Langer, personal communication, 2006). The new analysis of the recorded seismograms also reveals the presence of low-frequency components (4–5 s), which contribute to enhance the signal energy and could not be ascribed to a purely tectonic event. These new findings provide further evidence of the complexity of these events. Indeed, the examined earthquakes are a consequence of the tectonic deformation

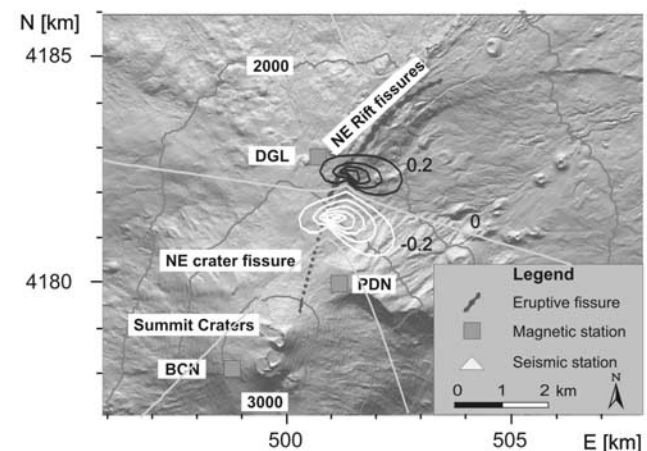


Figure 7. Contour map (at 0.2 nT intervals) of the expected piezomagnetic field change generated by the dip-slip fault model. The geometry and physical property of the fault are reported in Table 3.

exerted by the magmatic intrusion and this tectonic deformation could imply a much larger moment release than the single earthquake, which gives clues to the stress fields surrounding dike intrusions. The piezomagnetic field is likely to follow the deformation field and perhaps surge in magnitude at the time of an earthquake. Numerical models indicate that a dike propagating through the crust under significant magmatic overpressure can exert very high stress fields rising between 10 and 10^2 MPa [Gudmundsson, 2003]. Furthermore, high-pressure gas pulses, intimately involved with dike propagation, changing edifice geometry and access to the surface could trigger both seismic and aseismic failure. This would drop mean stress as observed and cause surface displacements as faults slip and fractures open. This could also trigger earthquakes. The difficulty is that there are no solid constraints supporting this. However, an estimate of the moment release generated around the dike intrusion is provided by the data from the long-base tilt station, installed at the volcanological observatory, Pizzi Deneri, near the PDN magnetic station. It showed changes of about $30 \mu\text{rad}$ in the tangential component and $15 \mu\text{rad}$ in the radial component in the time interval spanning the three main seismic events (Figure 6). It confirms a very high stress field at depth around the dike as magma pressure builds in the fracture zone until rupture occurs and the fracture propagates.

4. Discussion and Conclusions

[19] A quantitative interpretation of the observed coseismic magnetic changes is proposed based on an integrated analysis that combines the magnetic data with other seismological and geophysical observations. Strong magnetic transients were observed at the occurrence time of large seismic events whose magnitudes are greater than M3.8. To convincingly demonstrate the causality between magnetic variations and seismic events we verify the consistency and the correlation with other geophysical observations that independently reflect the state of the volcano. The epicentral migration toward the northeast suggested that the seismicity in the Northeast Rift is a consequence of dike propagation. Geophysical data interpretations point out that the changing stress field induced by the dike intrusion proportionally controls the seismicity rate during earthquake swarms. The seismicity related to the magma intrusion along the Northeast Rift indicated an abrupt stress change that could have triggered the earthquakes, reverse slip movements, and driven the magnetic changes. The magma intrusion clearly interacted with preexisting structures (Northeast Rift and Pernicana fault), which influenced the stress propagation and were reactivated during dike intrusion. Reverse dip-slip motion could be expected during the early stages of deformation as a mechanical consequence of differential uplift due to the dike intrusion [Acocella et al., 2004] and this would be enhanced by increased fluid/gas pressure. The modeling of the observed coseismic magnetic changes in terms of piezomagnetic mechanism clearly demonstrated the causal relation between crustal stress changes and local magnetic field changes. The coseismic piezomagnetic effects provided further evidence of the complex interaction between magma intrusions and tectonic response that took place during dike propagation along the Northeast Rift

zone. The results presented here encourage future studies on volcanomagnetic modeling with the aim of improving the understanding of volcano-tectonic processes.

[20] **Acknowledgments.** This study was performed with the financial support from the ETNA project (DPC-INGV 2004-2006 contract) and the VOLUME project (European Commission FP6-2004-Global-3). We are grateful to the Associate Editors Eduardo Del Pezzo and Stephen Park for their helpful comments. We thank Paul Davis and Antonio Meloni for constructive criticism that greatly improved the manuscript.

References

- Acocella, V., R. Funicello, E. Marotta, G. Orsi, and S. de Vita (2004), The role of extensional structures on experimental calderas and resurgence, *J. Volcanol. Geotherm. Res.*, *129*, 199–217.
- Aloisi, M., O. Cocina, G. Neri, B. Orecchio, and E. Privitera (2002), Seismic tomography of the crust underneath the Etna volcano, Sicily, *Phys. Earth Planet. Inter.*, *134*, 139–155.
- Aloisi, M., A. Bonaccorso, S. Gambino, M. Mattia, and G. Puglisi (2003), Etna 2002 eruption imaged from continuous tilt and GPS data, *Geophys. Res. Lett.*, *30*(23), 2214, doi:10.1029/2003GL018896.
- Aloisi, M., A. Bonaccorso, and S. Gambino (2006), Imaging composite dike propagation (Etna, 2002 case), *J. Geophys. Res.*, *111*, B06404, doi:10.1029/2005JB003908.
- Andronico, D., et al. (2005), A multi-disciplinary study of the 2002–03 Etna eruption: Insights into a complex plumbing system, *Bull. Volcanol.*, *67*, 314–330.
- Azzaro, R., M. S. Barbano, S. D'Amico, and T. Tuvè (2006), The attenuation of seismic intensity in the Etna region and comparison with other Italian volcanic districts, *Ann. Geophys.*, *49*(4/5), 1003–1020.
- Barberi, G., O. Cocina, V. Maiolino, C. Musumeci, and E. Privitera (2004), Insight into Mt. Etna (Italy) kinematics during the 2002–2003 eruption as inferred from seismic stress and strain tensors, *Geophys. Res. Lett.*, *31*, L21614, doi:10.1029/2004GL020918.
- Branca, S., D. Carbone, and F. Greco (2003), Intrusive mechanism of the 2002 NE-Rift eruption at Mt. Etna (Italy) inferred through continuous microgravity data and volcanological evidences, *Geophys. Res. Lett.*, *30*(20), 2077, doi:10.1029/2003GL018250.
- D'Amico, S., and V. Maiolino (2005), Local magnitude estimate at Mt. Etna, *Ann. Geophys.*, *48*, 2, 215–229.
- Del Negro, C., and G. Currenti (2003), Volcanomagnetic signals associated with the 2 001 flank eruption of Mt. Etna (Italy), *Geophys. Res. Lett.*, *30*(7), 1357, doi:10.1029/2002GL015481.
- Del Negro, C., and R. Napoli (2004), Magnetic field monitoring at Mt. Etna during the last 20 years, in *Mt. Etna: Volcano Laboratory*, *Geophys. Monogr. Ser.*, vol. 143, edited by A. Bonaccorso et al., pp. 241–262, AGU, Washington, D. C.
- Del Negro, C., R. Napoli, and A. Sicali (2002), Automated system for magnetic monitoring of active volcanoes, *Bull. Volcanol.*, *64*, 94–99.
- Del Negro, C., G. Currenti, R. Napoli, and A. Vicari (2004), Volcanomagnetic changes accompanying the onset of the 2002–2003 eruption of Mt. Etna (Italy), *Earth Planet. Sci. Lett.*, *229*(1–2), 1–14, doi:10.1016/j.epsl.2004.10.033.
- Evans, J. R., D. Eberhart-Phillips, and C. H. Thurber (1994), User's manual for simulps12 for imaging VP and VP/VS: A derivative of the "Thurber" tomographic inversion simul3 for local earthquakes and explosions, *U.S. Geol. Surv. Open File Rep.*, 94–431.
- Fenoglio, M. A., M. J. S. Johnston, and D. Byerlee (1995), Magnetic and electric fields associated with changes in high pore pressure in fault zones: Application to the Loma Prieta ULF emissions, *J. Geophys. Res.*, *100*, 12,951–12,958.
- Gudmundsson, A. (2000), Dynamics of volcanic systems in Iceland: Example of tectonism and volcanism at juxtaposed hot spot and mid-ocean ridge system, *Annu. Rev. Earth Planet. Sci.*, *28*, 107–140.
- Gudmundsson, A. (2003), Surface stress associated with arrested dykes in rift zones, *Bull. Volcanol.*, *65*, 606–619.
- Gudmundsson, A., and I. F. Loetveit (2005), Dike emplacement in a layered and faulted rift zone, *J. Volcanol. Geotherm. Res.*, *144*, 311–327.
- Hanks, T. C., and H. Kanamori (1979), A moment magnitude scale, *J. Geophys. Res.*, *84*, 2348–2350.
- Hough, S. E. (1996), Observational constraints on earthquake source scaling: Understanding the limits in resolution, *Tectonophysics*, *261*, 83–95.
- Johnston, M. J. (1997), Review of electric and magnetic fields accompanying seismic and volcanic activity, *Surv. Geophys.*, *18*, 441–475.
- Kanamori, H., and D. L. Anderson (1975), Theoretical basis of some empirical relations in seismology, *Bull. Seismol. Soc. Am.*, *65*, 1073–1095.
- Karakelian, D., S. L. Klemperer, A. C. Fraser-Smith, and G. A. Thompson (2002), Ultra-low frequency electromagnetic measurements associated

- with the 1998 M_w 5.1 San Juan Bautista, California earthquake and the implications for mechanism of electromagnetic earthquake precursors, *Tectonophysics*, 359, 65–79.
- Lanza, R., and A. Meloni (2006), *The Earth's Magnetism: An Introduction for Geologists*, 278 pp., Springer, Berlin.
- Mulargia, F., S. Tinti, and E. Boschi (1985), A statistical analysis of flank eruptions on Etna volcano, *J. Volcanol. Geotherm. Res.*, 23, 263–272.
- Murakami, H. (1989), Geomagnetic fields produced by electrokinetic sources, *J. Geomagn. Geoelectr.*, 41, 221–247.
- Obrizzo, F., F. Pingue, C. Troise, and G. De Natale (2001), Coseismic displacements and creeping along the Pernicana fault (Etna, Italy) in the last 17 years: A detailed study of a tectonic structure on a volcano, *J. Volcanol. Geotherm. Res.*, 109, 109–131.
- Okubo, A., and N. Oshiman (2004), Piezomagnetic field associated with a numerical solution of the Mogi model in a non-uniform elastic medium, *Geophys. J. Int.*, 159, 509–520.
- Patané, D., G. Barberi, O. Cocina, P. De Gori, and C. Chiarabba (2006), Time-resolved seismic tomography detects magma intrusions at Mount Etna, *Science*, 313, 821–823.
- Reasenber, P. A., and D. Oppenheimer (1985), FORTRAN computer programs for calculating and displaying earthquake fault-plane solutions, *U.S. Geol. Surv. Open File Rep.*, 85-379, 109 pp.
- Utsugi, M., Y. Nishida, and Y. Sasai (2000), Piezomagnetic potentials due to an inclined rectangular fault in a semi-infinite medium, *Geophys. J. Int.*, 140, 479–492.
- Zhao, S., R. D. Muller, Y. Takahashi, and Y. Kaneda (2004), 3-D finite-element modelling of deformation and stress associated with faulting: Effect of inhomogeneous crustal structures, *Geophys. J. Int.*, 157, 629–644, doi:10.1111/j.1365-246X.2004.02200.x.
- Zlotnicki, J., and J. L. Le Mouel (1990), Possible electrokinetic origin of large magnetic variations at La Fournaise volcano, *Nature*, 343, 633–635.
- Zlotnicki, J., and Y. Nishida (2003), Review on morphological insights of self-potential anomalies on volcanoes, *Surv. Geophys.*, 24, 291–338.

G. Currenti and C. Del Negro, Istituto Nazionale di Geofisica e Vulcanologia, Sezione di Catania, Piazza Roma 2, I-95123 Catania, Italy. (currenti@ct.ingv.it)

M. Johnston, U.S. Geological Survey, MS977, 345 Middlefield Road, Menlo Park, CA 94025, USA.

Y. Sasai, Disaster Prevention Division, Tokyo Metropolitan Government, Nishi-Shinjuku 2-8-1, Shinjuku-ku, Tokyo 163-8001, Japan.